Volume of supercooled water under pressure and the liquid-liquid critical point

Osamu Mishima[a)]
Polyamorphism Group, Exploratory Nanomaterials Research Laboratory, National Institute for Materials Science, 1-1 Namiki, Tsukuba 305-0044, Japan

(Received 28 June 2010; accepted 18 August 2010; published online 11 October 2010)

The volume of water (H_2O) was obtained at about 200–275 K and 40–400 MPa by using emulsified water. The plot of volume against temperature showed slightly concave-downward curvature at pressures higher than ≈200 MPa. This is compatible with the liquid-liquid critical-point hypothesis, but hardly with the singularity-free scenario. When the critical point is assumed to exist at ≈50 MPa and ≈223 K, the experimental volume and the derived compressibility are qualitatively described by the modified Fuentevilla–Anisimov scaling equation. © *2010 American Institute of Physics*. [doi:10.1063/1.3487999]

I. INTRODUCTION

According to the liquid-liquid critical-point (LLCP) hypothesis of water,[1] the liquid-liquid transition (LLT) is discontinuous, and the LLT line ends at the LLCP. Although the experimental and theoretical evidence suggests the existence of LLCP in supercooled water, crystallization makes absolute proof difficult, and the location of LLCP is uncertain.[2] Recently, the scaling theory for the general critical phenomenon was applied to the LLCP of water by Fuentevilla and Anisimov, and a parametric equation of state [Fuentevilla–Anisimov equation of state (FA-EOS)] was formulated.[3] Available experimental compressibility K_T, thermal expansion coefficient α_P, and heat capacity C_P seemed to follow the FA-EOS. However, because of the entire lack of volumetric data at low temperatures and high pressures, this agreement remained partial. Then, all of the available experimental results can also be qualitatively explained by the singularity-free (SF) scenario. According to the SF scenario,[4] the transition between the two liquids is always continuous. An experimental choice between the LLCP hypothesis and the SF scenario is desired, but it has been elusive. In this study, the specific volume V of supercooled water was obtained by using the emulsified liquid water, which can hinder the crystallization. When V of the emulsified water was regarded as that of pure water, it revealed not only the strongly varied liquid state at low pressures but also a slightly concave-downward change in the plot of volume against temperature at high pressures. These results support the LLCP hypothesis but not the SF scenario.

II. EXPERIMENT AND RESULT

About 1.3 cm^3 of water emulsion (water droplets 1–10 μm in size), made by stirring de-ionized H_2O (2000 mg) and a matrix (1000 mg methylcyclohexane, 1000 mg methylcyclopentane, and 100 mg sorbitan tristerate) with a homogenizer,[5,6] was closely sealed in an indium container of a fixed weight. After the weight of this sample was measured to an accuracy of 0.1 mg, it was compressed (and decompressed) in a steel cylinder (with an inner diameter of 15 mm) repeatedly at ~150 MPa/min. During the change in pressure, the temperature of the cylinder was kept constant by cold nitrogen gas and heater, and the displacement of the piston was measured to an accuracy of 1 μm. I note that the matrix hardly dissolves in water, and that the displacement-pressure curve is reproducible up to $\pm\sim 5$ μm, indicating no leakage of the liquid. I also note that even if the emulsion is used, the homogeneous nucleation of crystals occurs. Considering the friction between piston and cylinder, the pressure of the sample P was defined by the average of the compression pressure and the decompression pressure where the same displacement was observed; one-half of the difference between these pressures was used to correct P. The sample temperature T was determined to be $\pm\sim 2$ K from the cylinder temperature by establishing a relation between the two temperatures in separate experiments.

5–20 emulsion samples were compressed at each temperature. Additionally, compression of matrix samples without water and compression of indium containers were carried out in the same manner for correction. All samples were compressed up to a fixed P of ~440 MPa in order to avoid homogeneous nucleation of high-pressure ice and to simplify the correction of P.

By subtracting the average piston displacement of all "indium experiments" from the displacement of each "matrix experiment" at the same P-T condition, we can obtain the specific volume (volume par weight) of the matrix at P and T. Then, the average of the specific volumes obtained in all "matrix experiments" is calculated. The matrix's volume in any emulsion sample at P and T can be estimated from the weight of the matrix in the emulsion that is obtained by using the matrix/emulsion ratio of the sample weight. Here, uneven distribution of the surfactant (sorbitan tristerate) in the emulsion sample caused a slight ambiguity of the weight of the matrix. By subtracting the matrix's volume in each "emul-

a)Electronic mail: mishima.osamu@nims.go.jp.

sion experiment," we obtain the specific volume of pure water and then its compressibility at P and T. The averages for the volume, compressibility, pressure, and temperature of all the "emulsion experiments" in a small P-T area were calculated in order to obtain reasonable and reliable results from the scattered data; the mean values of V, K_T, P, and T are obtained, respectively. Note that no mathematical function is used to obtain these values.

Since the uncertainty in the matrix weight caused an error in V (estimated to be less than ~2%), all of the above-mentioned averages V are slightly shifted by a fixed value within its experimental uncertainty in order to be in accord with the known volume of water.[7] P and T are also shifted slightly in order to be in accord with the melting line (T_m line) of ice I_h, the homogeneous-nucleation line (T_H line) of ice I_h,[5,8] and the ice I_h-III transition line.[9] The occurrence of crystallization in liquid water was judged by examining whether a change in volume happened on the T_m line. Once crystallization occurred, the data of the sample were not used.

The experimental results of V and K_T are shown in Figs. 1(a) and 1(b). The red and orange points are the present data. Strictly speaking, V, which was obtained by using emulsified water, may be different from that of pure bulk water. Even so, the smoothness of the connection between the present V at low T and the literature data[10] at high T suggested that the V of this study could be regarded as that of pure bulk water. The present K_T also agreed with the literature data[11] reasonably in the region of overlap. As shown in Fig. 2(a), the lines of V at 0 and 100 MPa turn concave upward. As to the lines at 300 and 400 MPa, they are not as straight as they look. A careful inspection shows that they turn slightly concave downward at $P > \approx 200$ MPa and $T < \approx 250$ K. This may also be recognized by the tendency of the gradual negative-to-positive change in α_P at low T as P increases from 0 to 400 MPa. Since the volumetric experiment during cooling and heating at constant pressure has not been done in this study, the α_P values scattered due to the experimental error in T [Fig. 1(c)]. Nevertheless, the average of α_P in the high-P and low-T region in Fig. 1(c) is large, showing the existence of the minimum of $\alpha_P(T)$ at high P. The existence of the concave-downward property of $V(T)$ seems to be incompatible with the SF scenario because, as illustrated in Fig. 2(b), the V of the scenario is likely to change simply concave upward at these pressures. On the other hand, V of the LLCP hypothesis should be concave downward [Fig. 2(c)]. This is because V contracts more rapidly on the high-pressure side of LLCP as liquid water starts to separate quickly at low temperature. This concave-downward property is consistent with the connection between the high-density liquid (HDL) and the high-density amorphous ice (HDA), as shown by the thin broken line in Fig. 2(a).

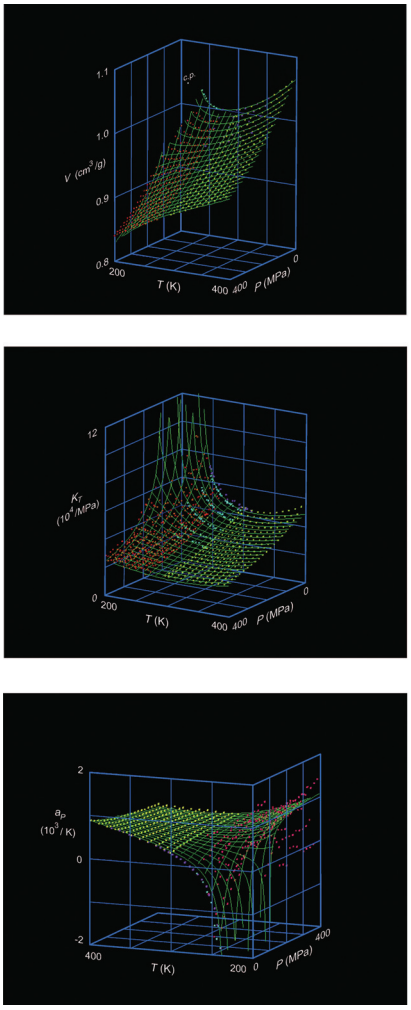

FIG. 1. The experimental (points) and theoretical (lines) V, K_T, and α_P of liquid H_2O. These figures can be rotated and the color of the background can be changed in the supplementary material (Ref. 28). Numerical values of V and K_T are also given in the material. (a) V—red and orange: this study; pink: Ref. 7; yellow: Ref. 10; and light blue: Refs. 12 and 13. c.p.: a possible LLCP (T_c=225 K, P_c=40 MPa, and V_c=1.04 cm^3/g). (b) K_T—red and orange: this study; yellow points are calculated by using the data in Ref. 10; pink: Ref. 14; and light blue: Ref. 11. K_T of the green lines becomes infinite at T_c=225 K and P_c=40 MPa. (c) α_P—red: this work; pink: Ref. 12; and yellow and light blue points are calculated by using the data in Refs. 10 and 13. In (a) and (b), the line of the red or orange points parallel to the pressure axis changes by ~5 K. The theoretical line changes by 10 K and 20 MPa.

III. CALCULATION OF EOS

The existence of LLCP is assumed, and it is examined whether the FA-EOS can reproduce the present experimental V and K_T. The theoretical V and K_T of water near LLCP can be written as $V=V(P,T)=V_{cr}+V_b$ and $K_T=K_T(P,T)=-(1/V)(\partial V/\partial P)_T=K_{T_{cr}}+K_{T_b}$. Here, $V_{cr}=V_{cr}(P,T)$ and $K_{T_{cr}}=K_{T_{cr}}(P,T)$ are the "critical" parts of V and K_T, respectively, and they are formulated in this study by following (and by modifying) the method of Fuentevilla and Anisimov.[3] I note that there is no qualitative improvement in the FA-EOS. $V_b=V_b(P,T)$ and $K_{T_b}=K_{T_b}(P,T)$ are the "(critical) background" parts of V and K_T. V_b is assumed to be a smooth and monotonous function of P and T, and K_{T_b} is calculated from V_b. The function of V_b is chosen arbitrarily in this study and has no physical meaning. V_b hardly affects the tendency of the pronounced changes in V and K_T near LLCP. Although V and K_T are the subjects of this paper, the theoretical α_P and C_P are also estimated. Parameters of the equations are fixed so that the theoretical values of V, K_T, α_P, and C_P are close to the corresponding available experimental values.[7,10,12–14,11,15–19]

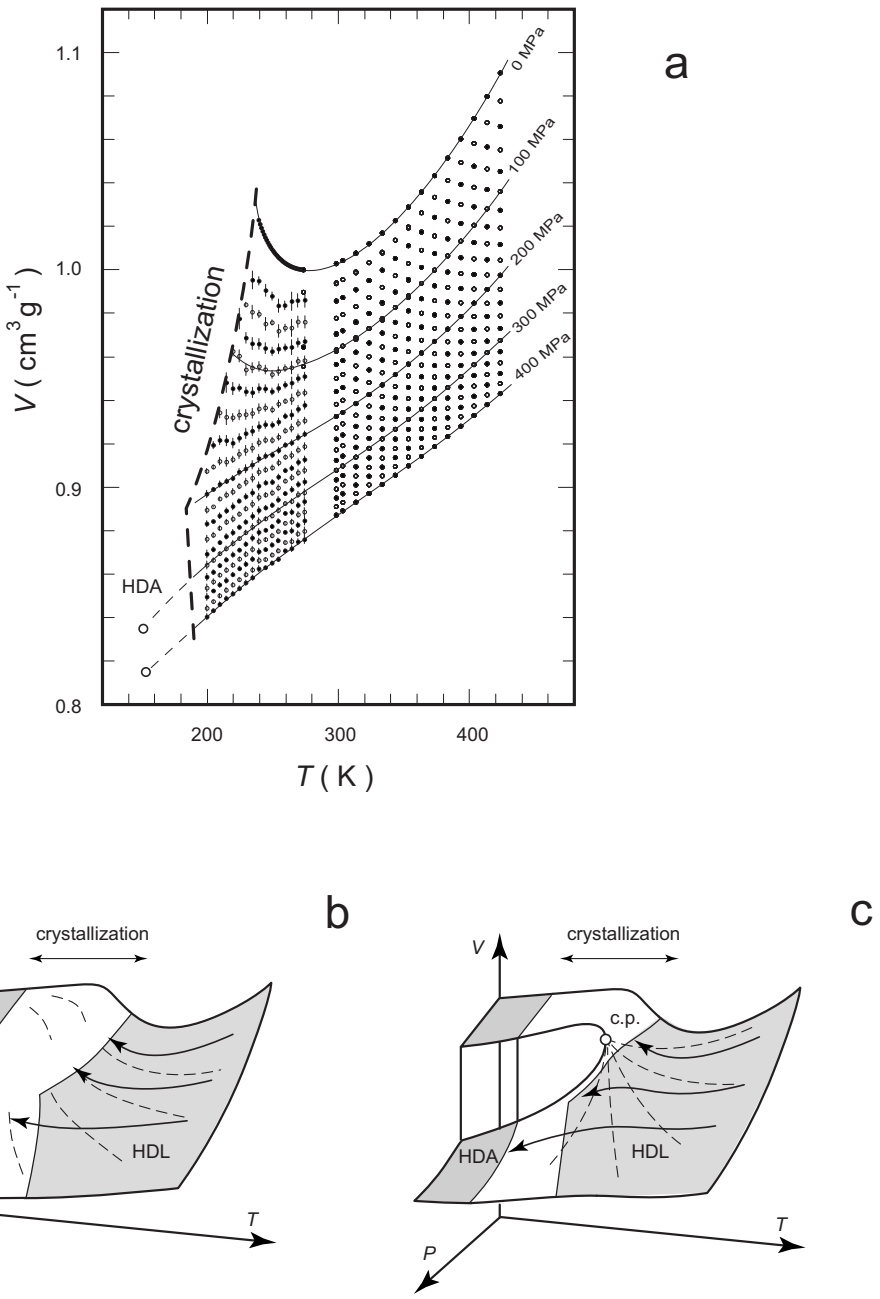

FIG. 2. The P-V-T relation of H_2O. (a) The experimental results. The points correspond to those in Fig. 1(a). Lines: for the eye, not theoretical lines. Two open circles of HDA are the V values of annealed high-density amorphous ice, which are estimated by using the data of Ref. 29. The low-T points at 20 MPa are missing. The small vertical line on each point at low T is the relative error of V of this study, and the absolute error of V at high T is smaller than the size of the point (Ref. 10). At high P, it is impossible to draw a line between 200 and 420 K, unless the line has the concave-downward curvature. (b) The SF scenario. (c) The LLCP hypothesis. In (b) and (c), the experimental data can be obtained in the gray regions.

Specifically, following Fuentevilla and Anisimov, we express the critical part G_{cr} of the Gibbs potential of water, $G=G(h_1,h_2)$, of two scaling fields, h_1 and h_2, by a scaling function f of one variable: $G_{cr}=G_{cr}(h_1,h_2) \approx h_2^{2-\alpha} f(h_1 h_2^{-\beta-\gamma})$, where $\alpha=0.109$, $\beta=0.326$, and $\gamma=1.239$ are the critical indices of the three-dimensional Ising model. We also employ the so-called "linear model" (Ref. 20) according to Fuentevilla and Anisimov. Then, by using the "polar" variables, r and θ, and system-dependent parameters, a and k, we can calculate h_1, h_2, and the first and second derivatives of G_{cr}: namely, $\phi_1=-\partial G_{cr}/\partial h_1$, $\phi_2=-\partial G_{cr}/\partial h_2$, $\chi_1=(\partial\phi_1/\partial h_1)_{h_2}$, $\chi_2=(\partial\phi_2/\partial h_2)_{h_1}$, and $\chi_{12}=(\partial\phi_1/\partial h_2)_{h_1}=(\partial\phi_2/\partial h_1)_{h_2}$ (Table I). I note that G_{cr} and its derivatives have units of J/g in the present calculations, although the units of these functions are usually defined as a dimensionless quantity.

Next, following Fuentevilla and Anisimov, we convert the coordinate (h_1,h_2) into the coordinate (P,T) (Table II, Fig. 3). The h_1 axis is a straight line in the P-T diagram, and the h_1 and h_2 axes intersect with each other at point (P_c,T_c), which is the pressure and temperature of LLCP. The h_2 axis corresponds to the transition line (LLT) between HDL and low-density liquid (LDL) and the line continuing from LLT (when extrapolated to the pressure lower than P_c). On the

TABLE I. The scaling fields and derivatives of G_{cr} after the linear model (Ref. 20).

Equation
$h_1=ar^{1.565}\theta(1-\theta^2)$
$h_2=r(1-1.361\theta^2)$
$\phi_1=kr^{0.326}\theta$
$\phi_2=akr^{0.891}(1.120-1.978\theta^2)-akr(1-1.361\theta^2)/3$
$\chi_1=(k/a)r^{-1.239}(1-0.474\theta^2)/c_0(\theta)$
$\chi_2=akr^{-0.109}(0.998+1.435\theta^2-0.904\theta^4)/c_0(\theta)-ak/3$
$\chi_{12}=kr^{-0.674}(-1.239\theta+0.589\theta^3)/c_0(\theta)$

$c_0(\theta)=1-0.100\theta^2-0.177\theta^4$. $r>0$. $-1\le\theta\le1$. The thermodynamic potential in Ref. 20 is regarded as the Gibbs energy in this study, and the critical indices of the three-dimensional Ising model are used.

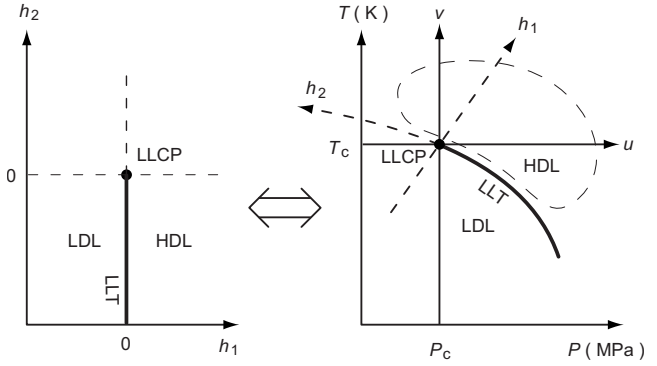

FIG. 3. The conversion of coordinate from (h_1,h_2) into (P,T) via (u,v). The LLT between HDL and LDL ends at LLCP. The FE-EOS is examined within the loop of the thin broken line in the right diagram.

premise that LDL crystallizes readily, LLT is regarded as the T_H line whose temperature at 0.1 MPa is ~232 K.[21] In this study, P of the T_H line (or LLT) is simply approximated by a quadratic function of T (~200 K$<T<$ ~240 K), although Fuentevilla and Anisimov approximated T of the T_H line to be a quadratic function of P. Therefore, the relation between P and T at $h_1=0$ corresponds the T_H line: $P(T)\approx c_1T^2+c_2T+c_3$. The three values, c_1-c_3, can be obtained from the available T_H experiments.[5,8] However, taking the experimental error of the location of the T_H line into account, its location was shifted in parallel in the P-T diagram; c_1-c_3 are thus parameters. Once the T_H line is fixed and when T_c is given, the value of P_c is calculated. V_c (cm^3/g) is the specific volume of water at LLCP and is a parameter. The slope of the h_1 axis (b_1 in Table II) is also a parameter. When T_c, c_1-c_3, V_c, and b_1 are given, P_c, a_1, and a_2 in Table II are calculated (Table III). Then, from Tables II and III, the relation between the (P,T) and (h_1,h_2) coordinates is obtained (Table IV).

By differentiating the composite function of $G_{cr}(h_1(P,T),h_2(P,T))$ with respect to P, we can write $V_{cr}=(\partial G_{cr}/\partial P)_T$ and $K_{T_{cr}}=-(1/V)(\partial V_{cr}/\partial P)_T$ by using ϕ_1, ϕ_2, χ_1, χ_2, and χ_{12} and by using the relation between the (h_1,h_2) and (P,T) coordinates (Table V). We can write $\alpha_{P_{cr}}$ and $C_{P_{cr}}$ in a similar way.

In short, once we give real values to r and θ, we can calculate the values of h_1, h_2, V_{cr}, and $K_{T_{cr}}$ (Table V), and then obtain the values of P and T from h_1 and h_2 (Table IV). By giving different values to r and θ, we can obtain $V_{cr}(P,T)$ and $K_{T_{cr}}(P,T)$ numerically.

As shown in Fig. 4, $V_b=V_b(P,T)$ is assumed to be a part of a "wide-tape-shaped" surface for convenience. The surface in one direction is written by a cubic equation, and that in another direction is written by a linear equation. Then, V_b can be expressed by using five parameters (d_1-d_5 in Table VI).

Combining the critical and "background" parts, we can calculate theoretical V and K_T. The parameters a, k, T_c, V_c, b_1, P_c (or c_1-c_3), and d_1-d_5 are set so that the theoretical values of the thermodynamic properties are close to the experimental values.

TABLE II. Conversion from the (h_1,h_2) coordinate to the (P,T) coordinate.

Equation	
(h_1,h_2) coordinate $\leftrightarrow$ (u,v) coordinate $\leftrightarrow$ (P,T) coordinate	
$h_1=u+a_1v+a_2v^2$	$u=V_c(P-P_c)/(R_WT_c)$
$h_2=v-b_1u$	$v=(T-T_c)/T_c$

The conversion is carried out through the (u,v) coordinate. $R_W=0.4619$ J/(g K) is the specific gas constant of water, and this satisfies the Clausius–Clapeyron equation.

IV. COMPARISON BETWEEN EXPERIMENT AND THEORY

The theoretical results are shown by the lines in Fig. 1. It is apparent that the experimental and theoretical values are reasonably close and that the more rapidly changing property around LLCP of the experiment and that of the theory resemble each other. The consistency between the theoretical and the experimental C_P values at 1 bar is shown by the thick green line in Fig. 5. As shown in Fig. 1(a), the theoretical EOS reproduces the concave-downward change in V at high P and low T. However, the agreement is not perfect quantitatively. Especially, the concave-downward curvature in V of the theory is stronger than that of the experiment at low T. The lines in Figs. 1 and 5 are an example where the parameters of the EOS are set so that apparently close similarities between experiment and theory are observed. Unfortunately, as for the present EOS, the precise scaling analysis of the similarity between the experiment and the theory was difficult without the experimental C_P values under P: namely, without the accurate Gibbs energy in the P-T diagram.

Regarding the parameters, T_c and P_c severely change the EOS immediately around LLCP. The parameters a, k, and b_1

TABLE III. Calculations of P_c, a_1, and a_2.

Equation
$P_c=c_1T_c^2+c_2T_c+c_3$
$a_1=-V_c(2c_1T_c+c_2)/R_W$
$a_2=-c_1V_cT_c/R_W$

It is because $P=(-a_2R_W/V_cT_c)T^2+[R_W(2a_2-a_1)/V_c]T-R_WT_c(a_2-a_1)/V_c+P_c$ (at $h_1=0$) corresponds to $P(T)\approx c_1T^2+c_2T+c_3$ of the T_H line.

TABLE IV. Calculations of P and T by using h_1 and h_2.

Equation
$P=(R_W T_c/V_c b_1)[\{(1/A)(b_1 h_1+h_2)+(B/2A)^2\}^{0.5}-h_2]-(R_W T_c/V_c b_1)(B/2A)+P_c$
$T=T_c\{(1/A)(b_1 h_1+h_2)+(B/2A)^2\}^{0.5}+T_c(1-B/2A)$
$A=-c_1 V_c T_c b_1/R_W$
$B=-V_c b_1(2c_1 T_c+c_2)/R_W+1$

generally affect the values around LLCP and V_c relates to the absolute values of the theoretical V. The five parameters of V_b affect the values in the region distant from LLCP relatively strongly. Therefore, the characteristic of the more rapidly changing behavior near LLCP is decided mainly by T_c, P_c, a, k, and b_1. The parameters in Fig. 1 are $a=b_1=1$, $k=3.9$, $T_c=225$ K, and $V_c=1.04$ cm^3/g. $P_c=40$ MPa, $a_1=12.99$, and $a_2=28.44$ are calculated from Table III by using $c_1=-0.05613$, $c_2=19.49$, and $c_3=-1504$. For the background part in Fig. 1, $d_1=7.2\times10^{-4}$, $d_2=3.4\times10^{-9}$, $d_3=-2.6\times10^{-7}$, $d_4=6.7\times10^{-4}$, and $d_5=22°$. The theoretical concave-downward property of V at high P and low T is not due to the background function.

V. LOCATION OF LLCP

P_c and T_c severely change the theoretical values of K_T, α_P, and C_P near LLCP. The LLCP location was changed, and these values were compared with the experimental values. In spite of a large number of the parameters of the present EOS, it is empirically found that the (P_c, T_c) location, which provides general agreement between theory and experiment, is in a certain range in the P-T diagram. Although numerical evaluation is difficult and the comparison is rough, when LLCP locates at the point of (×) in Fig. 6, apparently large discrepancies are observed near LLCP however other parameters may be changed; an improvement of one discrepancy causes another obvious discrepancy. The examples of the discrepancy are shown by the thin lines in Fig. 5. Therefore, the theory does not agree with the experiment if T_c is lower than ~205 K; the scaling function eliminates the possibility of low T_c proposed in Refs. 22 and 23, as well as the SF scenario.[4] When LLCP locates at point (○), there are rough resemblances between the theory and the experiment. When LLCP locates at point (●), ≈50 MPa and ≈223 K, there are closer resemblances: for example, the results in Figs. 1 and 5. This location (●) is close to the location estimated by Fuentevilla and Anisimov.[3] Additionally, the present location is coincident with those of other reports[24,25] and with that of a critical-point-like behavior suggested by the low-temperature extrapolation of the empirical EOS of high-T water.[26] T_c of H_2O is lower by several degrees than that of D_2O, which is suggested by the experiment of LLT of D_2O.[6]

TABLE V. Calculations of V_{cr}, $K_{T_{cr}}$, $\alpha_{P_{cr}}$, and $C_{P_{cr}}$.

Equation
$V_{cr}=(V_c/R_W T_c)(-\phi_1+b_1\phi_2)$
$K_{T_{cr}}=-(1/V)(V_c/R_W T_c)^2(-\chi_1+2b_1\chi_{12}-b_1^2\chi_2)$
$\alpha_{P_{cr}}=(1/VR_W T_c^2)\{-w\chi_1-(1-b_1 w)\chi_{12}+b_1\chi_2\}$
$C_{P_{cr}}=(T/T_c^2)(w^2\chi_1+2w\chi_{12}+\chi_2)$
$w=a_1+2a_2(T-T_c)/T_c$

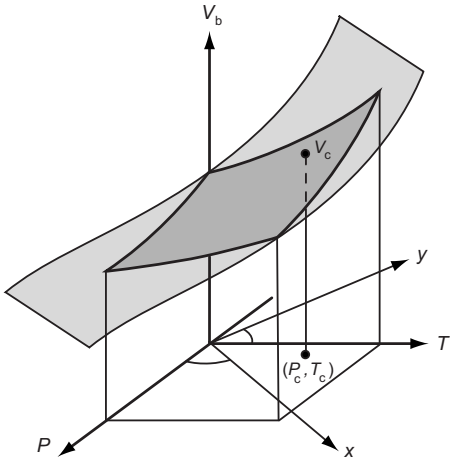

FIG. 4. The "band-shaped" $V_b(P,T)$ surface. For convenience, V_b along the y direction is written by a cubic equation and along the x direction by a linear equation.

VI. DISCUSSION AND CONCLUSION

Regarding the linear model, the intrinsic difference in K_T (and α_P) between LDL and HDL is ignored. Moreover, although the theory of the critical phenomena is usually valid in a very limited area around the critical point, it is applied to the wide HDL region (the loop of the thin broken line in Fig. 3), and the background function is made to fit for HDL. Therefore, the present EOS cannot be used in the LDL region. The difference between the thee-dimensional Ising exponents and the mean-field exponents affects the EOS near LLCP and near LLT at low temperatures where the present study was done. As noted by Fuentevilla and Anisimov,[3] the three-dimensional Ising exponents provided a better agreement than the mean-field exponents when the mean-field EOS of Ref. 27 was used.

The molecular-dynamics simulations are usually performed to predict the complex properties of water in various research fields. When the scaling EOS could be improved, these properties may be analyzed numerically by the scaling function.

TABLE VI. V_b and K_{T_b}.

Equation
$V_b\{x(P,T),y(P,T)\}=d_1 x+d_2 y^3+d_3 y^2+d_4 y+V_0$
$K_{T_b}\{x(P,T),y(P,T)\}=-(1/V)\{d_1\cos d_5-(3d_2 y^2+2d_3 y+d_4)\sin d_5\}$
$x(P,T)=P\cos d_5+T\sin d_5$
$y(P,T)=-P\sin d_5+T\cos d_5$
$V=V_{cr}+V_b$
Since $V_b(P_c,T_c)=V_c$, we obtain V_0 by using P_c, T_c, and V_c.

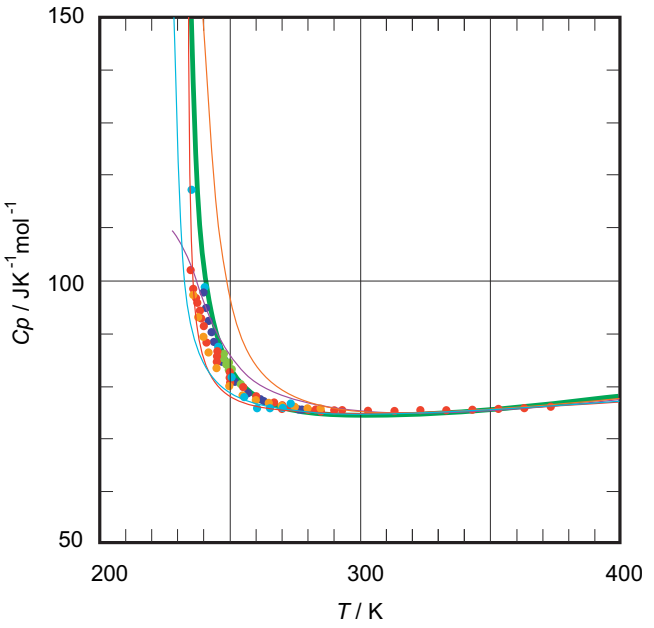

FIG. 5. The experimental (points) and theoretical (lines) C_P of water at 1 bar. The theoretical C_P is the sum of $C_{P_{cr}}$ and C_{P_b}, which are the critical and background parts of C_P, respectively. $C_{P_{cr}}$ of the thick green line is calculated by using the values of the parameters in Fig. 1, and the C_{P_b} (J K^{-1} mol^{-1}) is assumed to be a linear function of T (K): $C_{P_b}=57.6-0.054(T-225)$. The (P_c,T_c) point of the thick green line is (40 MPa, 225 K), and it locates at the mark (●) in Fig. 6. The other thin lines illustrate apparently no resemblance between the theory and the experiment. The (P_c,T_c) of these thin lines locates at the mark (×) in Fig. 6. Points: light blue (Ref. 15), red (Ref. 16), light green (Ref. 17), dark blue (Ref. 18), and orange (Ref. 19). The (P_c,T_c) of the thin lines: orange (70 MPa, 225 K), light blue (10 MPa, 225 K), violet (100 MPa, 205 K), and red (−50 MPa, 245 K). At high P, the theoretical C_P decreases as T decreases.

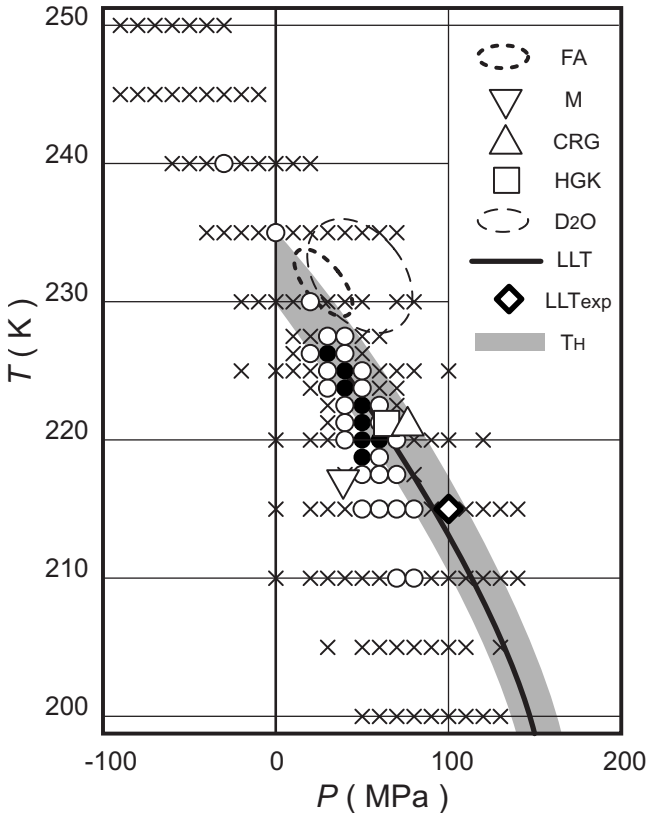

FIG. 6. Location of LLCP. If LLCP locates at a point of the marks (●), (○), and (×), the theoretical prediction and the experimental data show apparently close, rough, and no resemblance, respectively (see Fig. 5): FA (Ref. 3). M (Ref. 24). CRG (Ref. 25). HGK: the LLCP-like point of Ref. 26 as evaluated in Ref. 6. D_2O: LLCP of D_2O (Ref. 6). LLT: the LLT line in Fig. 1. LLTexp: the experimentally suggested LLT of H_2O (Ref. 5). T_H: the T_H line (Refs. 5 and 8). The reason of the small difference in the LLCP location between the Fuentevilla and Anisimov's work and this study is that Fuentevilla and Anisimov used the LLT line, which was located at a slightly higher T; our (○) point at 230 K corresponds to Fuentevilla and Anisimov's LLCP.

In conclusion, the present experimental results support the LLCP hypothesis rather than the SF scenario. The LLCP is roughly suggested to locate at ≈50 MPa and ≈223 K from the comparison between the available thermodynamic data and the modified FE-EOS.

ACKNOWLEDGMENTS

The author thanks Y. Suzuki for his useful comments.

[1] P. H. Poole, F. Sciortino, U. Essmann, and H. E. Stanley, Nature (London) **360**, 324 (1992).
[2] P. G. Debenedetti, J. Phys.: Condens. Matter **15**, R1669 (2003).
[3] D. A. Fuentevilla and M. A. Anisimov, Phys. Rev. Lett. **97**, 195702 (2006).
[4] S. Sastry, P. G. Debenedetti, F. Sciortino, and H. E. Stanley, Phys. Rev. E **53**, 6144 (1996).
[5] O. Mishima and H. E. Stanley, Nature (London) **392**, 164 (1998).
[6] O. Mishima, Phys. Rev. Lett. **85**, 334 (2000).
[7] G. S. Kell and E. Whalley, J. Chem. Phys. **62**, 3496 (1975).
[8] H. Kanno and C. A. Angell, J. Phys. Chem. **81**, 2639 (1977).
[9] G. S. Kell and E. Whalley, J. Chem. Phys. **48**, 2359 (1968).
[10] T. Grindley and J. E. Lind, Jr., J. Chem. Phys. **54**, 3983 (1971).
[11] H. Kanno and C. A. Angell, J. Chem. Phys. **70**, 4008 (1979).
[12] D. E. Hare and C. M. Sorensen, J. Chem. Phys. **84**, 5085 (1986).
[13] D. E. Hare and C. M. Sorensen, J. Chem. Phys. **87**, 4840 (1987).
[14] R. J. Speedy and C. A. Angell, J. Chem. Phys. **65**, 851 (1976).
[15] C. A. Angell, J. Shuppert, and J. C. Tucker, J. Phys. Chem. **77**, 3092 (1973).
[16] C. A. Angell, M. Oguni, and W. J. Sichina, J. Phys. Chem. **86**, 998 (1982).
[17] D. Bertolini, M. Cassettari, and G. Salvetti, Chem. Phys. Lett. **119**, 553 (1985).
[18] E. Tombari, C. Ferrari, and G. Salvetti, Chem. Phys. Lett. **300**, 749 (1999).
[19] D. G. Archer and R. W. Carter, J. Phys. Chem. B **104**, 8563 (2000).
[20] M. A. Anisimov, V. A. Agayan, and P. J. Collings, Phys. Rev. E **57**, 582 (1998).
[21] O. Mishima, J. Chem. Phys. **123**, 154506 (2005).
[22] H. Kanno and K. Miyata, Chem. Phys. Lett. **422**, 507 (2006).
[23] H. Kanno, K. Kajiwara, and K. Miyata, J. Chem. Phys. **132**, 194503 (2010).
[24] C. T. Moynihan, Mater. Res. Soc. Symp. Proc. **455**, 411 (1997).
[25] D. Corradini, M. Rovere, and P. Gallo, J. Phys. Chem. **132**, 134508 (2010).
[26] L. Haar, J. S. Gallagher, and G. S. Kell, *NBS/NRC Steam Tables* (Hemisphere, Washington, D.C., 1984).
[27] D. A. Fuentevilla, "A scaled parametric equation of state for the liquid-liquid critical point in supercooled water," MS thesis, University of Maryland, 2007.
[28] See supplementary material at http://dx.doi.org/10.1063/1.3487999 for the rotation of the three-dimensional figures and the numerical values (Fig. 1).
[29] C. G. Salzmann, T. Loerting, S. Klotz, P. W. Mirwald, A. Hallbrucker, and E. Mayer, Phys. Chem. Chem. Phys. **8**, 386 (2006).